Assessing energy balance via seismic and mechanical observations in high temperature induced crack damage in marbles

Heliyon 9 (2023) e19184

Contents lists available at ScienceDirect

Heliyon

journal homepage: www.cell.com/heliyon

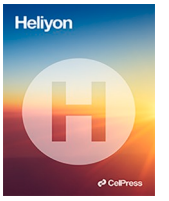

Assessing energy balance via seismic and mechanical observations in high temperature induced crack damage in marbles

Federico Vagnon [a,*], Sergio Carmelo Vinciguerra [b], Cesare Comina [b], Chiara Colombero [a], Anna Maria Ferrero [b], Roseane Missagia [c]

[a] Department of Environment, Land and Infrastructure Engineering, Politecnico di Torino, Torino, 10129, Italy
[b] Department of Earth Sciences, Università di Torino, Torino, 10125, Italy
[c] Universidade Estadual Norte Fluminense - Darcy Ribeiro, UENF, Laboratorio de Engenharia e Exploração de Petroleo, LENEP, 27925-535, Macaé, RJ, Brazil

ARTICLE INFO

Keywords:
Marbles
Thermal treatment
Physical and mechanical properties
Thermal crack damage

ABSTRACT

Assessing the rock physical and mechanical behavior under different temperatures has become of utmost importance. It is well known that thermal stresses induce significant crack damage in rocks due to thermal expansion or phase transformation and volume changes. Quantifying and forecasting the evolution of rock physical and mechanical parameters with temperature is thus crucial for evaluating rock integrity in many applications such as geothermal fields, nuclear waste storage, wildfire or volcanic processes. In marbles the degree of previous exposure to temperature and the chemical composition (i.e. calcite vs dolomite) plays a key role for controlling the mechanical evolution under temperature. Moreover separating out the energy contribution provided by anelastic processes driving crack damage and elastic reversible deformation under increasing temperature remains an open challenge. With these aims, three sample sets of marbles with different contents of calcite and dolomite from two Brazilian quarries were tested under different temperature conditions (from room temperature up to 600 °C). A marked increase of thermal cracking was observed after 400 °C, accompanying mass loss up to 1% and porosity increase. Moreover, a significant drop in seismic wave velocities, uniaxial compressive strength and electrical resistivity, in wet conditions, was also detected.

Spectral behavior from seismic traces and energy dissipation from stress-strain curves were analyzed. A dominance of the dissipated energy compared to the elastic one was observed and related to the generation of new fracturing surfaces. This hypothesis was supported by the spectral behavior showing multiple scattering effects in the high frequency components, with an increase in attenuation. The results suggested that the percentage of dolomite has a high influence on the mechanical behavior even at low temperature, mirroring the prevalence of brittle processes in dolomitic marbles. This study represents a comprehensive benchmark for the study of effect of temperature on rocks because of its multidisciplinary and multimethod approach and the demonstrated sensitivity to subtle textural changes. Moreover, it provides a reliable tool for crack damage analysis at each thermal stress.

* Corresponding author.
E-mail addresses: federico.vagnon@polito.it (F. Vagnon), sergiocarmelo.vinciguerra@unito.it (S.C. Vinciguerra), cesare.comina@unito.it (C. Comina), chiara.colombero@polito.it (C. Colombero), anna.ferrero@unito.it (A.M. Ferrero), rose@lenep.uenf.br (R. Missagia).

https://doi.org/10.1016/j.heliyon.2023.e19184
Received 3 February 2023; Received in revised form 22 March 2023; Accepted 15 August 2023
Available online 24 August 2023

List of symbols

c	Fitting parameter
c_i	Radius of the ith crack
E	Young's modulus, GPa
E_0	Dynamic Young's modulus, GPa
E*	Dynamic Young's modulus of the cracked material
F	Formation factor, dimensionless
n	Porosity, dimensionless or %
N	the total number of cracks embedded in the representative elementary volume V
P_0	Petrophysical reference value of each parameter
P(T)	Petrophysical value at temperature T
T	Temperature, °C
U	Strain energy density, dimensionless
U_e	Elastic strain energy density, dimensionless
U_d	Dissipated strain energy density, dimensionles
V_P	P-wave velocity, m/s
V_S	S-wave velocity, m/s
XRD	X-ray diffraction
XRF	X-ray fluorescence
ε_1	Axial deformation, dimensionless
ν_0	Dynamic Poisson ratio
ρ	crack density, dimensionless or 1/mm
σ_u	Uniaxial Compressive Strength, MPa

1. Introduction

Temperature is an important parameter for the characterization of rock masses because it drives mechanisms of degradation and weakening of the rock matrix [1]. In many geological and engineering purposes, such as geothermal exploitation and nuclear waste storage, the temperature plays a key role and, consequently, assessing its effects on the physical and mechanical properties is of utmost importance.

Many researchers have extensively studied the changes in physical and mechanics properties of rocks with respect to temperature [1–7].

The thermal damage of carbonates has become a topic of interest in the field of rock mechanics and engineering geology. Carbonates are usually involved in temperature-related applications (sometimes also related to anthropic activities) since they have a widespread diffusion in the Earth crust and are extensively used in cultural heritage artifacts and buildings. However the interplay between the heterogeneous nature of carbonates (grain size, cementation, deposition environment), the previous exposure to temperature and the complex recrystallizazion processes for marbles and the varying chemical composition (i.e. calcite vs dolomite) makes very difficult to forecast the mechanical evolution of these rocks under temperature and observe an unique behavior. Some researchers reported that the strength decreases with increasing temperature, the angle of internal friction increases first and then decreases with increasing temperature, and the cohesion trend is the opposite of the friction angle [7,8]. In other studies [1–7], the compressive strength was shown to increase up to a turning point temperature and then decrease exponentially.

Generally, the thermal degradation mechanism is a two-stage process: the initial thermal expansion increases stresses at the grain boundaries inducing crack initiation and propagation according to grain boundaries anisotropy and mechanical features. At higher temperature pervasive cracking is driven by increased mechanical stresses coupled with compositional and volume changes driven by different processes, such decalcination/decarbonation and/or mineral phase transition, leading to a physical and mechanical degradation [1,9–16]. In marbles, the calcitic and dolomitic phases involved in the metamorphism seem to control the response to thermal stresses. During their genesis, marbles already underwent to significant thermal gradients and consequently their secondary thermal damage is moderate compared to other carbonate rocks [17]. However, the primary thermal stress history can have a wide range of P/T metamorphic conditions that can affect the mechanical response to secondary thermal stresses. The parameters that could best describe secondary thermal stress for rocks already naturally thermally stressed, such as marbles, remain still an open question.

In previous works [1,17,18], we have analyzed the evolution of different parameters, such as porosity, ultrasonic pulse velocity and electrical resistivity, on marbles and limestones before and after high temperatures thermal treatments. However, the separation of the energy contribution provided by anelastic processes driving crack damage and elastic reversible deformation under increasing temperature remains an open challenge. With these aims, the same testing procedure was conducted on three types of marbles, collected in two Brazilian quarries, having different ratios of calcite and dolomite and a paragenesis corresponding to a different thermal stress history. A novel energy balance analysis was conducted to evaluate the percentage ratio between elastic and plastic energy during the thermal treatment by simultaneously analyzing the stress-strain curves during uniaxial compressive strength tests and the normalized spectra of the recorded seismic traces. Physical properties were complementary analyzed with mechanical ones; moreover, optical

observations on thin sections and crack densities were performed to assess the heating/cooling effects on rock microstructures. These observations, coupled to optical crack density estimation, allowed defining the rock behavior under different temperature levels. Furthermore, optical crack density was also compared to crack density derived from the Effective Medium Theory (EMT) [19], which allows linking the ultrasonic pulse velocity (UPV) degradation to the increase in thermal micro-fracturing.

2. Material and methods

2.1. Geological settings and sampling areas

Tested samples were collected in two different quarries (Carvalho and Sao Joaquim) located near the municipality of Italva (21°22′18″S, 41°41′26″O, Rio de Janeiro, Brazil), in the central area of the Ribeira Orogen [20], a Neo-Proterozoic orogenic system outcropping in the southeast of Brazil (Fig. 1a). The Italva klippe is a synformal structure with subparallel flanks and NE axis. It displays local migmatization and metamorphic conditions are related to medium to high amphibolite fácies [21].

Italva Marbles are comprised within the Metallurgical succession of the Italva Domain (Fig. 1b) where structural units of leucogranites and horneblende biotite gneiss include thick layers and veins of calcitic and dolomitic marbles with amphibolites [22]. In detail, the rock type outcropping in Sao Joaquim quarry belongs to the São Joaquim Unit and is a high-purity homogeneous marble, with sporadic presence of graphite and amphibolite intercalations [23], with a medium to coarse grain size. Marbles have formed as a result of contact metamorphism and metasomatism between a granitic cooling body and hosting rocks [24] which can occur in a wide range of temperatures and fluids circulation.

Three different sets of marble samples, with average diameter of 40 mm and height of 100 mm, where collected in the quarries. Two subsets of 6 samples were collected in Sao Joaquim quarry. The classification was based on grain size: coarse and medium grained marbles were respectively named “BRAZIL C″ and “BRAZIL SJ” (Fig. 1b). In Carvalho quarry, six homogeneous and medium grained marble samples, belonging to same São Joaquim Unit, were collected and named “BRAZIL D” (Fig. 1b).

2.2. Sample preparation and experimental methods

Mineral and oxides compounds of the three samples sets were evaluated by performing X-ray fluorescence (XRF) and diffraction (XRD) analyses on additional representative extra-samples belonging to the different sets. Results of these tests are listed in Table 1. Selected samples show transitional compositions and different percentage between calcite and dolomite: in particular, BRAZIL C and D have the same mineral composition (respectively 38% and 49% of calcite and 43% of dolomite for both the sets), whereas BRAZIL SJ is essentially dolomitic (73%). XRD also reveals that high temperature mineral compounds, i.e. forsterite and olivine are present in BRAZIL C and BRAZIL D, while low temperatures mineral compounds such wairauite and siderite are found in BRAZIL SJ. This

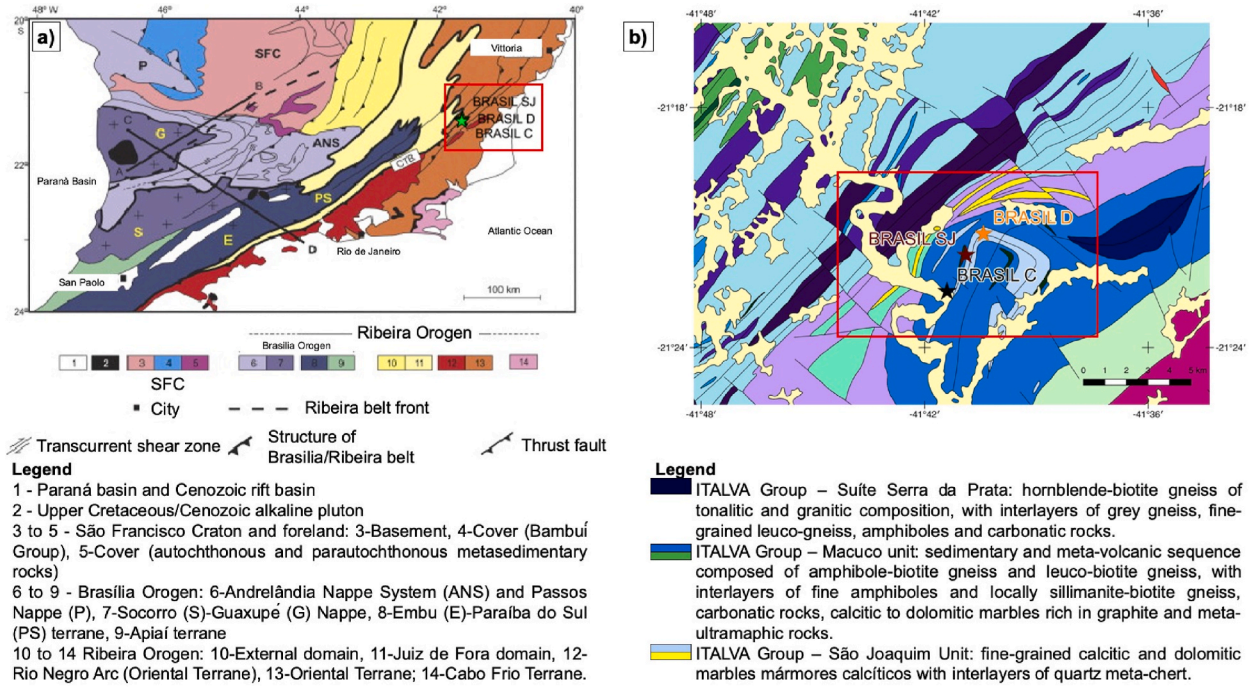

Fig. 1. a) Tectonic map of Brasilia and Ribeira orogenic belts and location of the sampling areas (modified after [22]. b) Geological map of the sampling area (modified after [25]).

Table 1
Percentage of mineral compounds and oxides retrieved from XRD and XRF analyses.

		Brazil C	Brazil D	Brazil SJ
	Compound name	Concentration [%]		
XRD	Calcite	37.9	48.98	14.84
	Quartz	–	–	–
	Dolomite	42.58	42.46	73.33
	Forsterite	18	–	–
	Tremolite	1.47	–	2.02
	Wairauite	0.05	–	4.61
	Siderite	–	–	5.18
	Olivine	–	8.1	–
XRF	MgO	17.33	20.39	21.36
	CaO	78.84	67.37	76.45
	SiO2	3.65	11.36	1.898
	AL2O3	–	0.54	–
	CoO	0.014	–	0.006
	Fe2O3	0.05	0.26	0.17
	Others	0.116	0.08	0.116

indicates a lower thermal stress environment for BRAZIL SJ associated to a higher level of dolomitization, likely due to metasomatism. In terms of grain size, BRAZIL C is the coarsest, with visible grains up to 2–3 mm.

For each sample, the same experimental procedure was followed:

1. Each sample was geometrically measured and weighed allowing samples densities to be evaluated.
2. Porosity (n), ultrasonic P- and S-wave velocity (V_P and V_S) and electrical resistivity (in saturated conditions, $\rho_{a,WET}$) were evaluated. Moreover, dynamic moduli (at low deformation) and formation factor (F, [26]) were estimated by combining density, seismic and electrical parameters.
3. For each set (Brazil C, D and SJ), rock specimens were divided into subsets of two samples and exposed to different target temperatures (200 °C, 400 °C and 600 °C respectively). The thermal treatment was a three-stage procedure: i) sample heating up to the target temperature with a heating rate of 0.06 °C/s; ii) 24-h sample exposure to constant target temperature; iii) slow-rate sample cooling down to room temperature (one day on average). More details are available in Ref. [1].
4. Normalized spectra contents of seismic signatures and multiparametric measurements at different treatment temperature described at (1) and (2) were repeated on each rock sample.
5 Mechanical properties were directly determined performing Uniaxial Compressive Strength (UCS) tests on threated samples. Uniaxial Compressive Strength (σ_u) and Young's modulus (E) were evaluated for each specimen.
6. The main effects of thermal treatment on the micro-structure of the studied marble rocks were quantified on 20 × 40 mm thin sections, directly obtained from natural and thermal treated (at target temperature of 600 °C) extra-samples belonging to the different sets.

Measured parameters, experimental equipment and international standards are listed in Table 2. Due to the limited number of samples, UCS tests were not performed on natural material at room temperature. However, reference parameters of the UCS in the natural material were provided by the quarry owners from several internal tests already performed. Also, previous studies performed by the authors ([1]) highlighted that there are no significant changes, in terms of Elastic modulus and UCS, in the stress-strain curve of carbonates at the lowest temperatures.

3. Results

Fig. 2 shows the variations of physical and mechanical parameters before and after thermal treatment at different target temperatures. Each parameter was evaluated firstly for each sample and then as an average over the samples subjected to the same thermal treatment. All shown data are associated to their standard deviations: where not visible, the length of the error bars is lower than the marker size. This low deviation from the average measured values guarantees the repeatability of the tests and justifies the relatively small number of specimens belonging to each class.

Thermal treatment induces significant changes in the physical and mechanical parameters of each specimen set. In particular, the increase in temperature does not almost induce mass loss (Fig. 2a) up to 400 °C (0.1% on average). With this respect, it must be also noted that tested samples were not dried before thermal treatment to not induce any thermal stresses during the drying procedure, which could lead to misinterpretation of the results. The mass loss up to 400 °C can be therefore imputed to water content loss and being this relatively constant an indication that the starting water content of the different samples was also almost constant. Above 400 °C, the mass loss instead increases till 1% denoting different effects on the rock structure.

Mass loss behavior is mirrored by an increase in open porosity (Fig. 2b). Porosity exhibits the same trend of mass loss up to 400 °C, with a slight increment from 0.0025 to 0.01; above 400 °C, porosity exponentially increases with values one order of magnitude greater.

Table 2
Experimental instruments, international standards and main physical parameters.

Physical property	International Standard	Test instrument	Technical parameters
Porosity, n	ISRM. Suggested methods for determining water content, porosity, density, absorption and related properties and swelling and slake-durability index properties. 1977	Caliper Analytical balance	Resolution: 0.0002 m Resolution: 0.0001 kg
P- and S-wave velocity, VP and VS	ASTM D2845-08 [27]	Ultrasonic pulse generation and acquisition system (Pundit Lab, Proceq)	Two cylindrical 250-kHz tx-rx probes
ER measurement	–	Syscal-Pro (Iris instruments) acquisition system	On-purpose built measuring quadrupole ([21])
Heat treatment	–	Carbolite Temperature programmer Eurotherm 2416CG	Temperature range: 1100 °C Heating rate: 0.06 °C/s Resolution: 1 °C
Mineral composition	–	XRD: S2 Phaser (Bruker Company) XRF: S2 Ranger (Bruker Company)	
UCS	ISRM. Suggested methods for determining the Uniaxial Compressive Strength and Deformability of Rock Materials. 1977 [28]	MTS apparatus (MTS System Corporation)	Load cell: 250 kN Strain rate:1 μm/s
Microscopic observations and microphotographs	–	Transmitted polarized light microscope and camera	Open-source image processing program ImageJ [29]. Moreover, the pre- and post-heating crack length was measured using the ImageJ plugins "Analyze Skeleton" [30]

The increase in mass loss and open porosity produces a detectable decrease in ultrasonic pulse velocity (UPV) (Fig. 2c and 2d), both for P- and S-wave measurements. P- and S-wave velocity trends agree with the hypothesis of crack damage within the rock medium because of thermal cracking, which progressively slowed the ultrasonic wave first arrival time at each step of temperature. However, while porosity and mass loss do not change significantly up to 200 °C, the overall seismic parameters show a clear decrease already at this temperature level.

Formation factor trend over temperatures (Fig. 2e), also highlights this drop around 200 °C and a progressive reduction of saturated apparent electrical resistivity of rock samples. This behavior agrees with the Sauer's theory [31] identifying the main possible path of electrical current in porous medium through the interstitial fluid. Consequently, the cracks generated by thermal treatment cause an increase in the rock overall porosity, that once saturated by water, acts as an electrical conductor.

By regression analysis, it was found that exponential relationships best fitted the experimental data for all the investigated parameters. As shown in Table 3, the proposed relationships are under the form:

$$P(T) = P_0 e^{\pm cT} \tag{1}$$

where P_0 is the petrophysical reference value of each parameter and c is a fitting parameter, depending on the specific rock structure and rock degradation effect, with the sign of the exponent being positive if the considered parameter increases with temperature (negative if it decreases with temperature). Results are in good agreement with previous studies on marbles [1,3,4,12,16–18,32–37].

The variation of UCS (Fig. 2f) was moderate until a temperature of 400 °C, with a small increase between 20 °C and 200 °C. This UCS increase is supported by an increase in axial deformation as a function of temperatures. Indeed, the stress-strain curves (Fig. 3) show an increase in deformation for temperatures greater than 400 °C, that could indicate strain hardening driven from the brittle to ductile transition, in accordance with previous studies [1,15,17]. The increase of axial strain up to 200 °C also confirms the hypothesis of material strengthening (increase in UCS values) due to the competition of mechanical compaction carried by the closure of pre-existing cracks and dilatant hardening due to the opening of freshly formed cracks. Moreover, dolomite (see Table 1) appears to

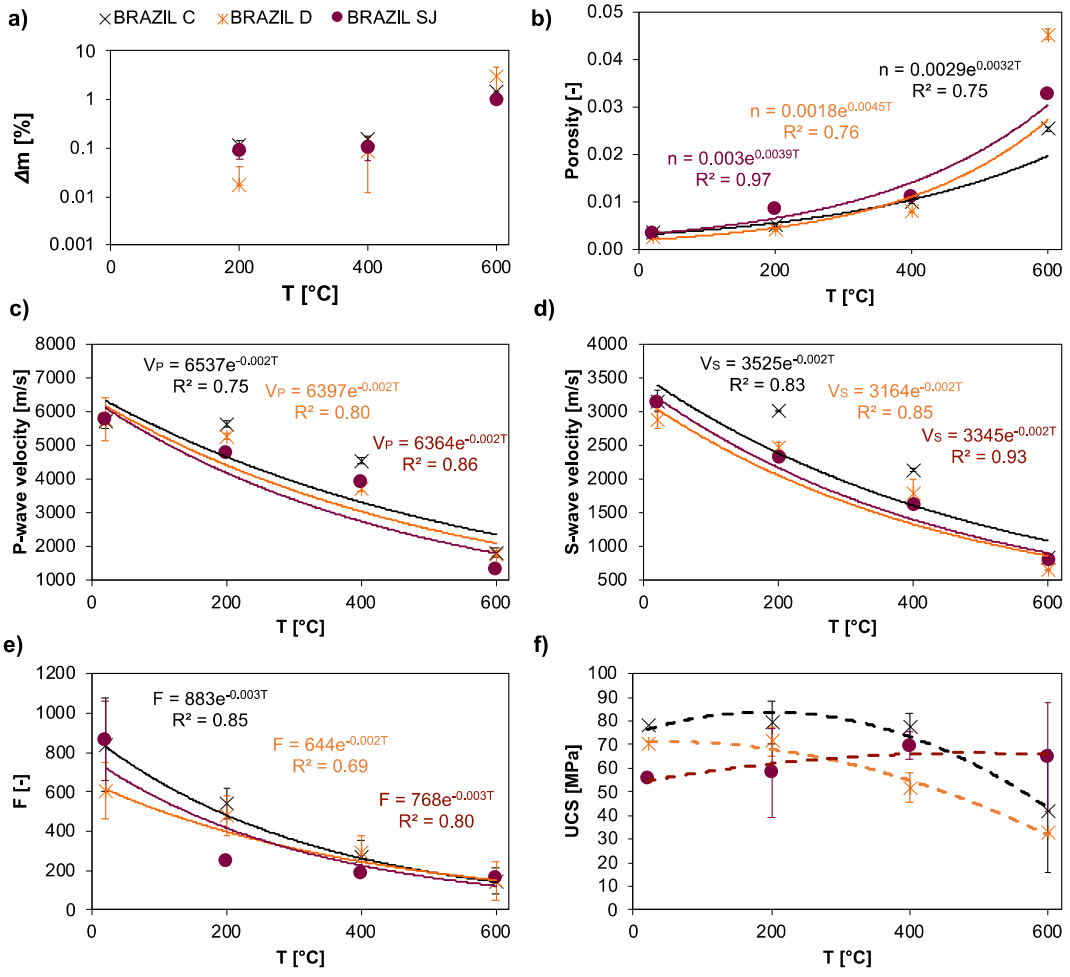

Fig. 2. Relationships between temperature and a) mass loss, b) porosity, c-d) P- and S- wave velocity, e) formation factor and f) UCS values measured on each sample set.

strengthen rocks at low temperature, while it should be expected the opposite, being the dolomite prone to decomposition at lower temperatures then calcite [14].

Except for relatively high BRAZIL SJ UCS values at 600 °C, the analyzed marbles have comparable maximum axial deformations at the same temperature target. Physical and mechanical results are listed in Table 1A in Appendix A.

4. Discussion

Thermal crack damage is recorded in all tested marbles. At temperatures lower than 400 °C, the anisotropic thermal expansion coefficient of crystallographic principal axes of calcite grains [38,39] induces inter-grain stresses, which cause the initiation and propagation of cracks. In fact, calcite is known to expand on heating much more in the direction of its optical axis than perpendicular to it. Since the individual grains are oriented randomly, the result is a springing apart of contiguous grains, giving rise to a non-zero residual stress state inside the material. Consequently, when mechanical actions are applied, the appearance of the microcracks reveal that the key role is mainly played by the resistance of the crystals. When temperature is higher than 400 °C, the process of calcite and dolomite decomposition is triggered (at around 550 °C), causing microcracks and voids formation between and inside bigger grains. Moreover, porosity increase might be likely related to the combination of grain crushing and crack damage [14]. The decalcination and decarbonation process can be self-limited upon decreasing oxygen fugacity [40] and increasing confinement on the rock [41,42].

To quantitatively verify and demonstrate these theories, microscopic observations were performed on natural samples and after thermal treatment at the highest temperature, i.e. 600 °C, for all investigated samples. Microscopic analyses supported the interpretation of the micromechanical damage induced by heating. Fig. 4 compares representative microphotographs of thin sections and highlights how the temperature increase generated a shift of the crack length cumulative distribution to higher values, particularly evident in BRAZIL C but partially noticeable for all the specimens, coherently with the increase in pore voids at 600 °C and the calcite decomposition processes, which lead to reduction of the physical and mechanical parameters within this range of temperature. In BRAZIL SJ this effect appears to be less significant given the reduced calcite content of this set of samples. Optical crack density on thin sections was measured via ImageJ code, highlighting and confirming the higher thermal degradation with increasing target temperature.

Crack density can be also estimated from UPV values [43], by inverting the elastic wave velocity field into a non-dimensional crack density, defined as:

$$\rho = \frac{1}{V}\sum_{i=1}^{N} c_i^3 \tag{2}$$

where c_i is the radius of the ith crack and N the total number of cracks embedded in the representative elementary volume V.

Assuming that changes in dynamic elastic properties are correlated to the amount of crack damage, we can apply an Effective Medium Theory (EMT), assuming a 'no stress interaction approximation' and neglecting the stress interactions complexity between cracks. By doing this, effective dynamic elastic moduli of a cracked solid can be calculated on the crack orientations and distribution solely [19,44]. For a random crack center and orientation distribution (isotropic), stress interactions are partially compensating geometrically and the effective dynamic Young's modulus E* of a dry rock can be written as:

$$\frac{E_0}{E^*} = 1 + \frac{16\left(1-\nu_0^2\right)\left(1-\frac{3\nu_0}{10}\right)}{9\left(1+\frac{\nu_0}{2}\right)}\rho \tag{3}$$

where E_0 and ν_0 are the dynamic Young's modulus and Poisson ratio of the uncracked material and E* is the dynamic Young's modulus of the cracked material, calculated by UPV measurements.

Table 4 and Fig. 5 compare the dimensionless crack density and the normalized optical crack density as a function of temperature. Both crack density values show an increase at high temperatures. Moreover, the dimensionless crack density trend highlights the previously presented mass loss and porosity evolution over temperatures (Fig. 2a and 2b). Indeed, the increase in effective porosity is due to an increase in crack density, with consequent mass loss after grain crushing and decalcination and decarbonation triggering.

These results strengthen the hypothesis of formation and propagation of thermally induced microcracks, and generated inter and intra grain boundaries damage via comminution and crushing, mirrored by an overall reduction in the values of physical parameters with increasing heating temperature. Obviously, optical analyses carried out in 2D via microphotographs of thin sections are not representative of the whole volume of the analyzed rock samples. It is also difficult to compare two parameters estimated with different

Table 3
Fitting parameters for physical characteristics of the three analyzed marble sets.

Set	N			V_P			V_S			F		
	P_0 [-]	C	R^2	P_0 [m/s]	C	R^2	P_0 [m/s]	c	R^2	P_0 [-]	c	R^2
BRAZIL C	0.0029	0.0032	0.75	6537	−0.002	0.75	3525	−0.002	0.83	883	−0.003	0.85
BRAZIL D	0.0018	0.0045	0.76	6397	−0.002	0.8	3164	−0.002	0.85	644	−0.002	0.69
BRAZIL SJ	0.003	0.0039	0.97	6346	−0.002	0.86	3345	−0.002	0.93	768	−0.003	0.8

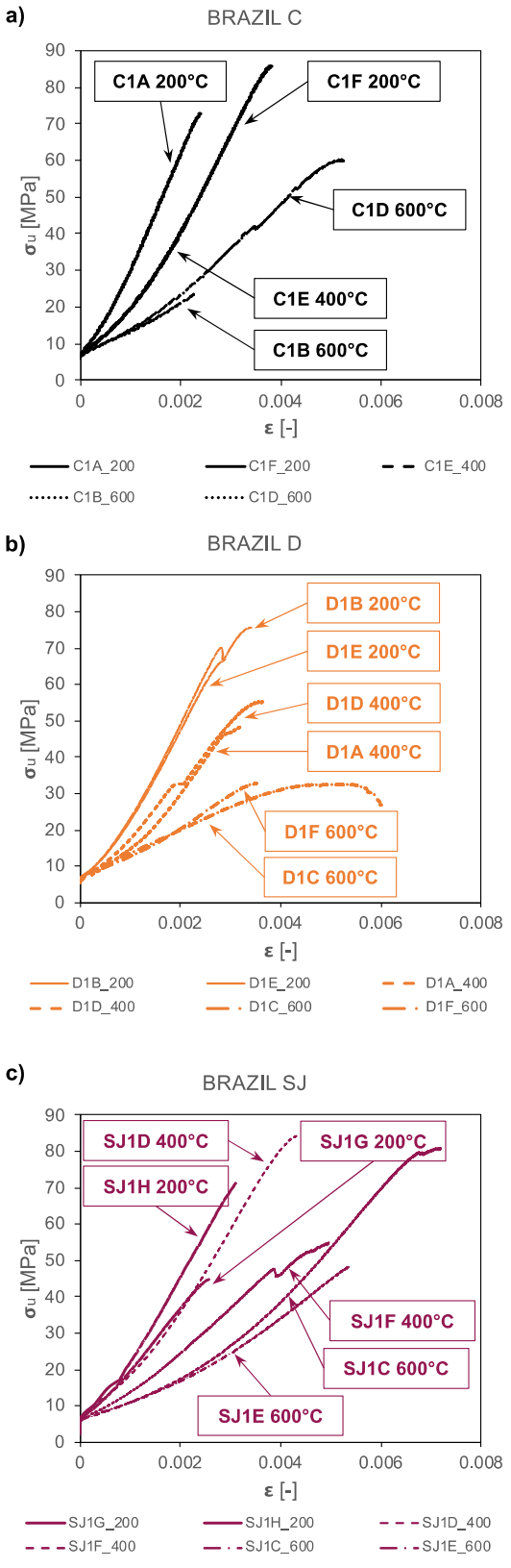

Fig. 3. Marble stress-strain curve for a) BRAZIL C, b) BRAZIL D and c) BRAZIL SJ samples.

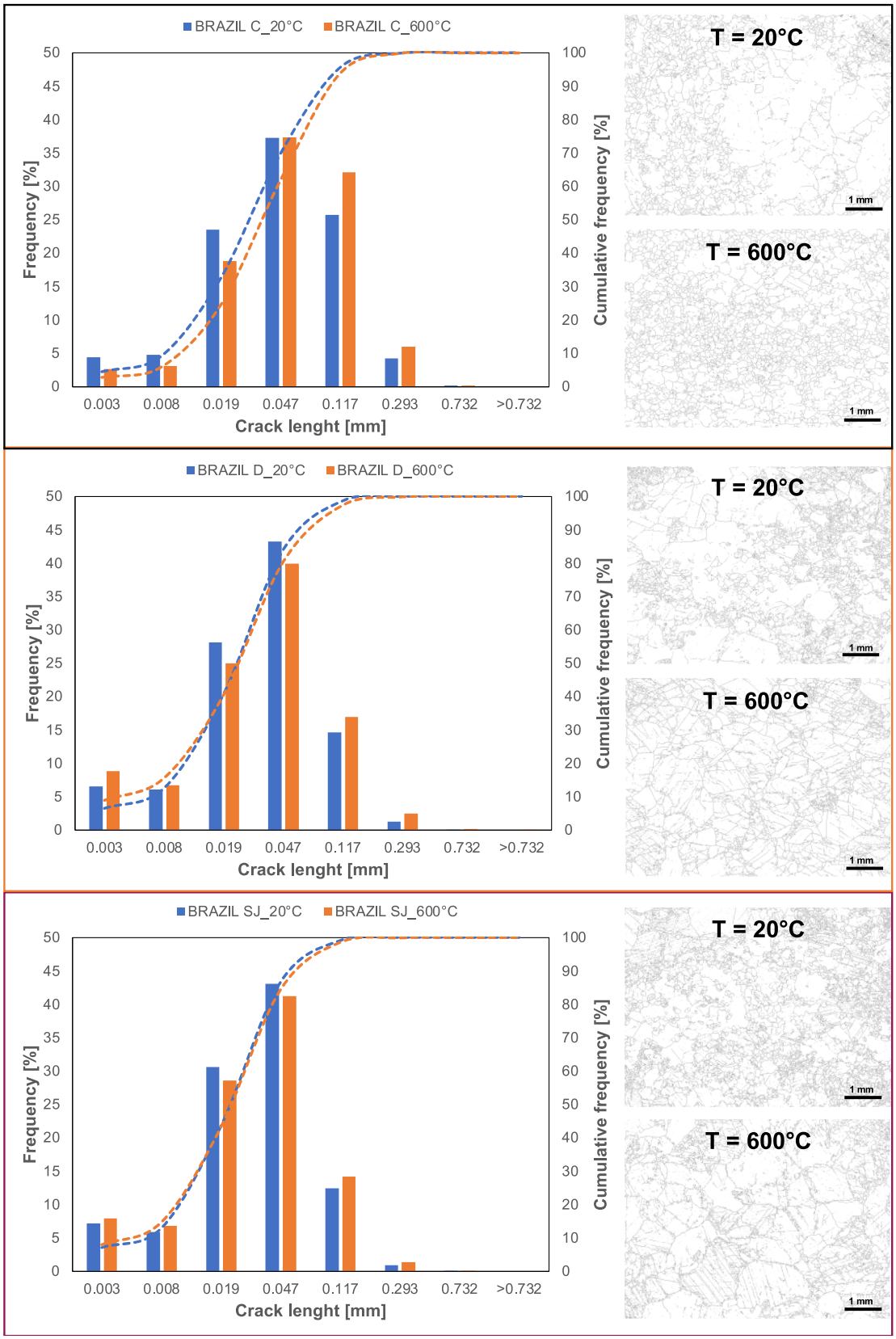

Fig. 4. Frequency (column bars) and cumulative (dashed lines) distribution of crack length for each sample at 20 °C (blue) and at 600 °C (orange).

methods and dimensions, given that only end members were available for optical observations. Nevertheless the performed considerations appear clear in delineating the rock behaviour under increasing temperature.

For the above reasons, further analyses were also performed for defining the characteristic energy of marbles after temperature treatment. The area under the stress-strain curves is called the strain energy density, U, and is commonly separated into the elastic (U_e) and the dissipated (U_d) strain energy density. These strain energy densities are given by:

$$U = \int \sigma_1 d\varepsilon_1 = \sum_{i=1}^{n} \frac{1}{2}(\sigma_{1i} + \sigma_{1i-1})(\varepsilon_{1i} + \varepsilon_{1i-1}) \tag{4}$$

$$U_e = \frac{\sigma_u^2}{E} \tag{5}$$

$$U_d = U - U_e \tag{6}$$

Based on these equations, the percentage variation of accumulated elastic energy and dissipated energy at different target temperatures were calculated for each sample set. Fig. 6 shows the variation of elastic and dissipated energy over temperatures for each marble set. In general, an increase of dissipated energy can be observed as temperature increase. In the 400–600 °C range, this increase is more marked (up to 80%) compared to previous temperature stages. Below 200 °C, the amount of elastic energy accumulated before reaching the peak stress for BRAZIL C and D is higher than the dissipated one, confirming the textural integrity and a very low thermal damage. However, BRAZIL SJ shows a dominance of dissipated energy, even at 200 °C, suggesting that its dolomitic texture (and Mg presence in the compound) is more prone to dissipate energy at low temperatures, even with a negligible mass loss (respectively red and green lines in Fig. 6). This can also be explained by the lower thermal stress history of BRAZIL SJ, thus being more sensitive and prone to crack damage formation and energy dissipation upon thermal stresses at low temperatures. Upon increasing temperature, there is a moderate decrease in elastic energy up to 400 °C, which becomes more marked at higher temperatures, in agreement with the other physical and mechanical analyses previously discussed.

At present, ultrasonic waves mostly focus on the analysis of variations in P and S waves velocities through first arrival picking. However, it has been observed that also the spectrum characteristics of acquired signals may have a correlation with the degree of rock damage. Particularly it has been noted (e.g. Refs. [6,45]) that crack formation and propagation can have a significant attenuation effect on the high frequency content of ultrasonic waves. Therefore, the analysis of the spectral content of ultrasonic waves could be a further parameter to highlight thermal crack damage.

In Fig. 7 the average normalized spectra of the acquired traces at the different treatment temperature levels are reported for the three sets of samples. A progressive loss of the high frequency content and a systematic shift of the maxima of the spectra towards the lower frequencies can be observed for increasing treatment temperature. The loss in the high frequency spectral content is particularly clear at temperatures higher than 400 °C with a narrowing of the spectral shape and a remarkable attenuation of frequencies higher than 250 KHz. This spectral behavior reflects the progressive increase in crack density that promotes increased scattering, and consequent higher attenuation of the high frequency components, acting as a filter. It can also be noted that this filtering effect is more relevant in all sets of samples for the 600 °C treatment temperature, while treatment temperatures of 200 °C and 400 °C represent a transition zone. This behavior is particularly clear for BRAZIL C, the coarsest marble with the highest grain size, and partially observable also in the other samples sets. This also indicates a wavelength/grain size dependency, as the loss of the high frequency content and the shift of the spectra towards lower frequencies for the coarser samples is the highest.

5. Conclusions

A multiparametric analysis of laboratory tests on three sets of marbles collected in two Brazilian quarries was performed to investigate the variation of a suite of several physical and mechanical parameters as a function of varying temperatures. The following conclusions were drawn:

Table 4
EMT parameters for the evaluation of dimensionless crack density from UPV and normalized optical crack density values.

Set	T [°C]	E_{dyn} [GPa]	SD_E_{dyn} [GPa]	ν [−]	SD_ν [−]	ρ [−]	SD_ρ [−]	normalized ρ_optical [−]
BRAZIL C	20	70	11	0.28	0.05	0	0	1
	200	65	2	0.30	0.01	0.06	0.11	
	400	34	1	0.36	0.01	0.80	0.24	
	600	5	0	0.37	0.03	9.42	1.48	1.33
BRAZIL D	20	63	10	0.33	0.05	0	0	1
	200	47	4	0.36	0.02	0.27	0.10	
	400	25	7	0.35	0.04	1.28	0.24	
	600	4	0	0.42	0.01	13.92	3.15	1.10
BRAZIL SJ	20	73	6	0.29	0.03	0	0	1
	200	42	2	0.35	0.01	0.57	0.06	
	400	21	2	0.40	0.01	1.90	0.03	
	600	5	0	0.22	0.01	11.46	0.82	1.28

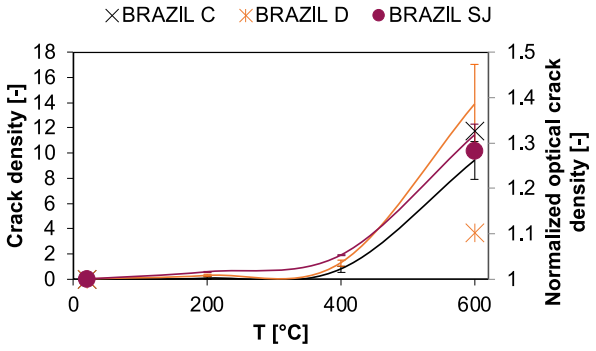

Fig. 5. Normalized crack densities determined optically (right y-axis) and crack density from UPV (left y-axis) measurements versus temperature.

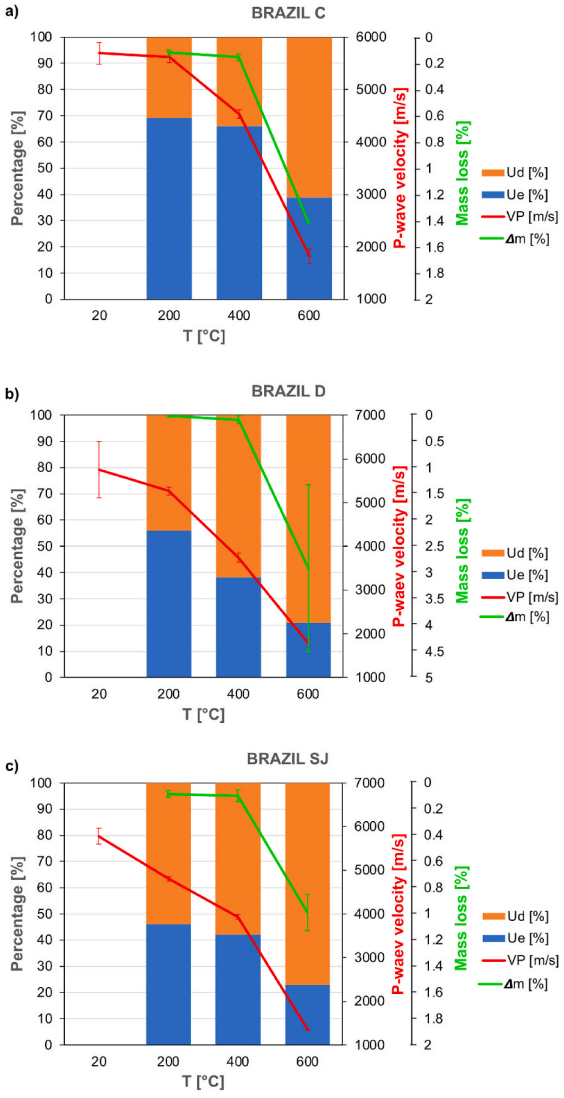

Fig. 6. Energy dissipation and elastic energy percentage of each analyzed marble set at various treatment temperatures, compared to P-wave velocity (red line) and mass loss (green line) trends.

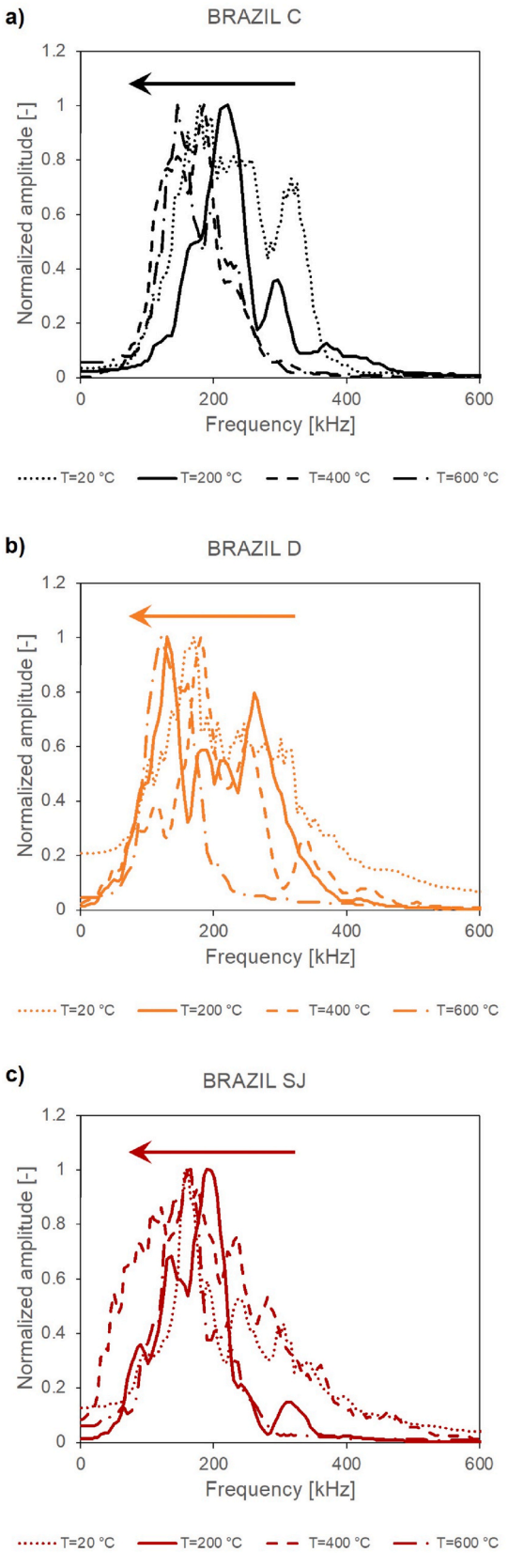

(caption on next page)

Fig. 7. Spectral content at different treatment temperature levels for a) BRAZIL C, b) BRAZIL D and c) BRAZIL SJ samples.

- For the studied rock samples, the thermal crack damage increase after 400 °C, accompanying mass loss up to 1%. Increased porosity is mirrored by a significant drop in UPV, F and UCS values. Exponential relationships were fitted to the trends of physical parameters versus temperature.
- From the analyses of seismic normalized spectra and stress-strain curves, the dissipated energy becomes dominant (80% on average) compared to the elastic one at high temperatures, highlighting the work done for creating new fracturing surfaces, in good agreement with the observation made on thin sections.
- The incremental crack generation and energy dissipation is also highlighted by the ultrasonic spectral behavior that shows multiple seismic scattering in the high frequency components, with an increase in attenuation.

The relative percentages of calcite and dolomite play a crucial role in the above described processes. Marbles with higher dolomitic percentage show a dominance of dissipated energy, even at low temperatures, suggesting that the dolomitic texture is more prone to brittle processes. Summarizing, two mechanisms are triggered by thermal treatment in marbles, in agreement with processes observed for carbonates. However, the extent of the mechanisms appears controlled by the intrinsic nature of the recrystallization in marble and the percentage of dolomite involved: at low temperature, the anisotropic deformation of calcite grains induces moderate intergranular stresses that concurs to the formation and propagation of microcracks. At high temperatures, above 400 °C, the thermal stress overcome calcite grain resistance, inducing an increase in open porosity with a consequent, even if modest, detectable mass loss. Moreover, despite the previous thermal history of marbles during their formation, decomposition processes still occur at around 550 °C and concur to increase open porosity due to the formation of new voids space, mirrored by a slight mass loss.

This study represents a comprehensive benchmark for the study of effect of temperature on rocks because of its multidisciplinary and multimethod approach and the demonstrated sensitivity to subtle textural changes. Future developments will focus on investigating different cooling phases (e.g water), heating-cooling cycles and coupling the effect of confining pressure to temperature.

Author contribution statement

Federico Vagnon; Chiara Colombero: Conceived and designed the experiments; Performed the experiments; Analyzed and interpreted the data; Contributed reagents, materials, analysis tools or data; Wrote the paper.

Sergio Carmelo Vinciguerra; Cesare Comina; Anna Maria Ferrero; Roseane Missagia: Conceived and designed the experiments; Analyzed and interpreted the data; Contributed reagents, materials, analysis tools or data; Wrote the paper.

Data availability statement

Data included in article/supplementary material/referenced in article.

Additional information

No additional information is available for this paper.

Funding

This research did not receive any specific grant from funding agencies in the public, commercial, or not-for-profit sectors. Open access funding provided by Politecnico di Torino within the CRUI-CARE Agreement.

Declaration of competing interest

The authors declare that they have no known competing financial interests or personal relationships that could have appeared to influence the work reported in this paper.

Acknowledgements

N. Fusi and F. Agliardi at the Department of Earth and Environmental Sciences, University of Milan Bicocca are warmly thanked for the mechanical tests carried out.

Appendix A

Table 1A
Physical and mechanical results as a function of temperature for each analyzed set.

Set	T [°C]	Δm [%]	SD [%]	n [−]	SD_n [−]	V_P [m/s]	SD_V_P [m/s]	V_S [m/s]	SD_V_S [m/s]	V_P/V_S [−]	SD_V_P/V_S [−]	F [−]	SD_F [−]	from mechanical tests			
														σ_c [MPa]	SD [MPa]	E [GPa]	SD [GPa]
BRAZIL C	20			0.003	0.0001	5692	211	3151	152	1.83	0.11	838	237	78		32	
	200	0.12	0.02	0.005	0.0001	5623	105	3006	16	1.99	0.03	539	76	79	9	30	4
	400	0.15	0.02	0.010	0.0002	4528	79	2139	21	2.19	0.05	271	85	78	6	27	3
	600	1.41	0.01	0.025	0.0005	1819	136	836	16	1.94	0.04	146	67	42	26	24	2
BRAZIL D	20			0.002	0.0001	5750	644	2884	132	1.94	0.30	604	144	70		33	
	200	0.02	0.02	0.004	0.0001	5263	92	2471	76	2.04	0.07	478	99	71	6	31	2
	400	0.09	0.07	0.008	0.0001	3736	105	1796	190	2.26	0.29	290	86	52	6	26	3
	600	2.91	1.58	0.045	0.0011	1785	85	665	4	2.07	0.03	146	96	33	0	22	3
BRAZIL SJ	20			0.003	0.0001	5780	179	3131	63	1.85	0.08	862	202	56		37	
	200	0.09	0.02	0.008	0.0001	4804	54	2335	30	2.07	0.05	252	23	58	19	36	14
	400	0.10	0.05	0.011	0.0002	3931	53	1627	68	2.45	0.17	189	17	70	6	25	3
	600	0.99	0.14	0.033	0.0004	1355	6	808	9	1.71	0.02	162	13	65	23	23	1

References

[1] F. Vagnon, C. Colombero, F. Colombo, C. Comina, A.M. Ferrero, G. Mandrone, S.C. Vinciguerra, Effects of thermal treatment on physical and mechanical properties of Valdieri Marble - NW Italy, Int. J. Rock Mech. Min. Sci. 116 (2019) 75–86, https://doi.org/10.1016/j.ijrmms.2019.03.006.

[2] S. Chaki, M. Takarli, W.P. Agbodjan, Influence of thermal damage on physical properties of a granite rock: porosity, permeability and ultrasonic wave evolutions, Construct. Build. Mater. 22 (2008) 1456–1461, https://doi.org/10.1016/j.conbuildmat.2007.04.002.

[3] R.D. Dwivedi, R.K. Goel, V.V.R. Prasad, A. Sinha, Thermo-mechanical properties of Indian and other granites, Int. J. Rock Mech. Min. Sci. 45 (2008) 303–315, https://doi.org/10.1016/j.ijrmms.2007.05.008.

[4] Y. Zhao, Z. Wan, Z. Feng, D. Yang, Y. Zhang, Q. Fang, Triaxial compression system for rock testing under high temperature and high pressure, Int. J. Rock Mech. Min. Sci. 52 (2012) 132–138, https://doi.org/10.1016/j.ijrmms.2012.02.011.

[5] Y.L. Chen, J. Ni, W. Shao, R. Azzam, Experimental study on the influence of temperature on the mechanical properties of granite under uniaxial compression and fatigue loading, Int. J. Rock Mech. Min. Sci. 56 (2012) 62–66, https://doi.org/10.1016/j.ijrmms.2012.07.026.

[6] S. Liu, J. Xu, Mechanical properties of Qinling biotite granite after high temperature treatment, Int. J. Rock Mech. Min. Sci. 71 (2014) 188–193, https://doi.org/10.1016/j.ijrmms.2014.07.008.

[7] J. Yang, L.Y. Fu, W. Zhang, Z. Wang, Mechanical property and thermal damage factor of limestone at high temperature, Int. J. Rock Mech. Min. Sci. 117 (2019) 11–19, https://doi.org/10.1016/j.ijrmms.2019.03.012.

[8] Q.B. Meng, J.F. Liu, Hu Pu, Y. Wu, C.K. Wang, Mechanical properties of limestone after high-temperature treatment under triaxial cyclic loading and unloading conditions, Rock Mech. Rock Eng. 54 (2021) 6413–6437, 10.1007/s00603-021-02638-1.

[9] D.P. Jansen, S.R. Carlson, R.P. Young, D.A. Hutchins, Ultrasonic-imaging and acoustic emission monitoring of thermally-induced microcracks in lac-du-bonnet-granite, J. Geophys. Res. Solid Earth 98 (1993) 22231–22243.

[10] T. Funatsu, M. Seto, H. Shimada, K. Matsui, M. Kuruppu, Combined effects of increasing temperature and confining pressure on the fracture toughness of clay bearing rocks, Int. J. Rock Mech. Min. Sci. 41 (2004) 927–938, https://doi.org/10.1016/j.ijrmms.2004.02.008.

[11] Z. Abdulagatova, I.M. Abdulagatov, V.N. Emirov, Effect of temperature and pressure on the thermal conductivity of sandstone, Int. J. Rock Mech. Min. Sci. 46 (2009) 1055–1071, https://doi.org/10.1016/j.ijrmms.2009.04.011.

[12] H. Yavuz, S. Demirdag, S. Caran, Thermal effect on the physical properties of carbonate rocks, Int. J. Rock Mech. Min. Sci. 47 (2010) 94–103, https://doi.org/10.1016/j.ijrmms.2009.09.014.

[13] V. Brotóns, R. Tomás, S. Ivorra, J.C. Alarcón, Temperature influence on the physical and mechanical properties of a porous rock: san Julian's calcarenite, Eng. Geol. 167 (2013) 117–127.

[14] M.J. Heap, S. Mollo, S. Vinciguerra, Y. Lavallée, P. Baud, D.B. Dingwell, G. Iezzi, F.W. von Aulock, Thermal weakening of the carbonate basement under Mt. Etna volcano (Italy): implications for volcano instability, J. Volcanol. Geoth. Res. 250 (2013) 42–60, https://doi.org/10.1016/j.jvolgeores.2012.10.004.

[15] A. Castagna, A. Ougier-Simonin, P.M. Benson, J. Browning, R.J. Walker, M. Fazio, S. Vinciguerra, Thermal damage and pore pressure effects of the brittle-ductile transition in comiso limestone, J. Geophys. Res. Solid Earth 123 (2018) 7644–7660, https://doi.org/10.1029/2017JB015105.

[16] J. Peng, G. Rong, M. Cai, M.D. Yao, C.B. Zhou, Physical and mechanical behaviors of a thermal-damaged coarse marble under uniaxial compression, Eng. Geol. 200 (2016) 88–93, https://doi.org/10.1016/j.enggeo.2015.12.011.

[17] F. Vagnon, C. Comina, A.M. Ferrero, S.C. Vinciguerra, C. Colombero, G. Mandrone, Temperature induced damage in marble rocks: correlations with physical and mechanical properties, in: 55th U.S. Rock Mechanics/Geomechanics Symposium 2021, vol. 2, 2021, 175961.

[18] F. Vagnon, C. Colombero, C. Comina, A.M. Ferrero, G. Mandrone, R. Missagia, S.C. Vinciguerra, Relating physical properties to temperature-induced damage in carbonate rocks, Géotech. Lett. 11 (2021) 1–11, https://doi.org/10.1680/jgele.20.00122.

[19] M.H.B. Nasseri, A. Schubnel, R.P. Young, Coupled evolutions of fracture toughness and elastic wave velocities at high crack density in thermally treated Westerly granite, Int. J. Rock Mech. Min. Sci. 44 (2007) 601–616, https://doi.org/10.1016/j.ijrmms.2006.09.008.

[20] F.F.M. Almeida, G. Amaral, U.G. Cordani, K. Kawashita, The precambrian evolution of the south American cratonic margin south of amazonas river, in: The Ocean Basin and Margins (Naim & Stille, Eds.), vol. 1, Plenum, New York, 1973, pp. 411–446.

[21] C. Peixoto, M. Heilbron, Geologia da Klippe Italva na regiao entre Cantagalo e Itaocara, Nordeste do Estado do Rio dei Janeiro, São Paulo, UNESP, Geociências 29 (3) (2010) 277–289.

[22] M. Heilbron, B. Machado, Timing of terrain accretion in the Neoproterozoic-Eopaleozoic Ribeira orogen (SE Brazil), Precambrian Res. 125 (2003) 87–112.

[23] J.J. Batista, B.S. Gomes, C.M.L. Marchetto, L.A.M. Costa, Estado do Rio de Janeiro. Secretaria de Estado de Industria, Comercio e Turismo. Departamento de Recursos Minerais. Projeto Carta Geológica do Estado do Rio de Janeiro Folha de Italva, Relatório final – 1, 2010, pp. 1–88 (in Portuguese).

[24] L.S.S. Costa Filho, B.P. Duarte, Estudo do metamorfismo de contato resultante da interacao entre magmas graniticos e marmores da regiao de Italva, Norooeste do Estado do Rio de Janeiro, 49° Congresso Brasileiro de Geologia, 2018. Rio de Janeiro, 20-24 August (in portuguese).

[25] B.P. Duarte, M. Tupinambà, J.R. Nogueire, M. Heilbron, J.C. Horta de Almeida, Mapa Geologico Folha ITAPERUNA SF-24-V-C-I CPRM. 2009, 2009 (in portuguese).

[26] G.E. Archie, The electrical resistivity log as an aid in determining some reservoir characteristics, SPE Repr. Ser. 9 (1942), https://doi.org/10.2118/942054-g. –16.

[27] ASTM D2845-08, Standard Test Method for Laboratory Determination of Pulse Velocities and Ultrasonic Elastic Constants of Rock, ASTM, International (American Society for Testing and Materials), West Conshohocken, Pennsylvania, USA, 2008.

[28] ISRM, Suggested Methods for Determining Water Content, Porosity, Density, Absorption and Related Properties and Swelling and Slake-Durability Index Properties, 1977.

[29] C.A. Schneider, W.S. Rasband, K.W. Eliceiri, NIH Image to ImageJ: 25 years of image analysis, Nat. Methods 9 (7) (2012) 671–675, https://doi.org/10.1038/nmeth.2089. PMID: 22930834; PMCID: PMC5554542.

[30] I. Arganda-Carreras, R. Fernández-González, A. Muñoz-Barrutia, C. Ortiz-De-Solorzano, 3D reconstruction of histological sections: application to mammary gland tissue, Microsc. Res. Tech. 73 (2010) 1019–1029, https://doi.org/10.1002/jemt.20829.

[31] M.C. Sauer Jr., P.E. Southwick, K.S. Spiegler, M.R.J. Wyllie, Electrical conductance of porous plugs: ion exchange resin-solution system, Ind. Eng. Chem. 47 (1955) 2187–2193.

[32] A.M. Ferrero, P. Marini, Technical note: experimental studies on the mechanical behaviour of two thermal cracked marbles, Rock Mech. Rock Eng. 34 (2001) 57–66, https://doi.org/10.1007/s006030170026.

[33] M. Lion, F. Skoczylas, B. Ledésert, Effects of heating on the hydraulic and poroelastic properties of bourgogne limestone, Int. J. Rock Mech. Min. Sci. 42 (2005) 508–520, https://doi.org/10.1016/j.ijrmms.2005.01.005.

[34] M.Y. Koca, G. Ozden, A.B. Yavuz, C. Kincala, T. Onargand, K. Kucukd, et al., Changes in the engineering properties of marble in fire-exposed columns, Int. J. Rock Mech. Min. Sci. 43 (2006) 520–530, https://doi.org/10.1016/j.ijrmms.2005.09.007.

[35] K. Malaga-Starzec, U. Åkesson, J.E. Lindqvist, B. Schouenborg, Microscopic and macroscopic characterization of the porosity of marble as a function of temperature and impregnation, Construct. Build. Mater. 20 (2006) 939–947, https://doi.org/10.1016/j.conbuildmat.2005.06.016.

[36] W.S. González-Gómez, P. Quintana, A. May-Pat, F. Avilés, J. May-Crespoa, J.J. Alvarado-Gil, Thermal effects on the physical properties of limestones from the Yucatan Peninsula, Int. J. Rock Mech. Min. Sci. 75 (2015) 182–189, https://doi.org/10.1016/j.ijrmms.2014.12.010.

[37] G. Musso, R.M. Cosentini, S. Foti, C. Comina, G. Capasso, Assessment of the structural representativeness of sample data sets for the mechanical characterization of deep formations, Geophysics 80 (2015) D441–D457, https://doi.org/10.1190/GEO2014-0351.1.

[38] J.L. Rosenholtz, D.T. Smith, Linear Thermal Expansion of Calcite, Var. Iceland Spar, and Yule Marble, Am. Mineral, 1949.

[39] W.H. Ito, A.M. Ferrero, F. Vagnon, M.R. Migliazza, P.I.B. de Queiroz, Thermomechanical numerical analysis of bowing in marble slabs, in: Rock Mechanics for Natural Resources and Infrastructure Development - Proceedings of the 14th International Congress on Rock Mechanics and Rock Engineering, ISRM, 2020, 2019.

[40] S. Mollo, M.J. Heap, G. Iezzi, K.U. Hess, P. Scarlato, D. Dingwell, Volcanic edifice weakening via decarbonation: a self-limiting process? Geophys. Res. Lett. (2012) https://doi.org/10.1029/2012GL052613.
[41] R.R. Bakker, M.E.S. Violay, P.M. Benson, S.C. Vinciguerra, Ductile flow in sub-volcanic carbonate basement as the main control for edifice stability: new experimental insights, Earth Planet Sci. Lett. 430 (2015) 533–541, https://doi.org/10.1016/j.epsl.2015.08.017.
[42] F. Parisio, S. Vinciguerra, O. Kolditz, T. Nagel, The brittle-ductile transition in active volcanoes, Sci. Rep. (2019), https://doi.org/10.1038/s41598-018-36505-x.
[43] O. Nishizawa, Seismic velocity anisotropy in a medium containing oriented cracks: transverse isotropy case, J. Phys. Earth 30 (1982) 331–347.
[44] P.M. Benson, P.G. Meredith, A. Schubnel, Role of void space geometry in permeability evolution in crustal rocks at elevated pressure, J. Geophys. Res. Solid Earth 111 (2006), https://doi.org/10.1029/2006JB004309.
[45] S.D. Goodfellow, M. Ghofranitabari, M.B. Nasseri, Evaluation of wave propagation properties during a truetriaxial rock fracture experiment using acoustic emission frequency characteristics, in: American Geophysical Union, Fall Meeting 2013, 2013.